Park *et al. Applied Biological Chemistry* (2024) 67:33
https://doi.org/10.1186/s13765-024-00883-w

KSABC
The Korean Society for Applied Biological Chemistry

ARTICLE

Open Access

Correlation analysis between artemisinin and its derivative contents and trichome characteristics from different *Artemisia* species

Yun Ji Park[1], To Quyen Truong[1,2], Yeong Bin Choi[1], Phuong Kim Huynh[1,2], Jinyoung Moon[1], Song Yi Koo[3], Hyoung Seok Kim[1] and Sang Min Kim[1,2*]

Abstract

Artemisia species have significant commercial, medical, and economic value and are widely used in the traditional medicine and pharmaceutical industries. Artemisinin, a powerful antimalarial agent, is an important pharmaceutical metabolite that primarily accumulates within the glandular trichomes (GTs) on the leaf surface of *Artemisia* plants. Trichomes arising from the elongation of epidermal cells can be classified into GTs and non-glandular trichomes (NGTs) based on their morphology. GTs and NGTs are present in *Artemisia* species, and the relationship between GTs and artemisinin has been extensively studied; however, the correlation between NGTs and artemisinin remains relatively unexplored. In this study, we inferred artemisinin derivatives and trichome characteristics based on the type of species, developmental stage, and leaf age and conducted correlation analyses to investigate the factors influencing artemisinin content across different *Artemisia* species. Artemisinin and its derivatives exhibited variations in distribution based on species and leaf age, with a decreasing trend observed across most species as the developmental stage progressed. Noticeable differences among *Artemisia* species were observed in leaf shape, morphology, and trichome distribution. Although the observed data did not evidently differentiate between species, developmental stage, and leaf age groups, principal component analysis revealed that artemisinin was positively associated with the NGTs density, indicating a correlation coefficient of 0.56 ($p < 0.0001$). Therefore, the number of NGTs may affect the artemisinin content in different *Artemisia* species.

Keywords *Artemisia* species, Artemisinin, Glandular trichome, Non-glandular trichome, Correlation analysis

Introduction

Artemisia, a genus belonging to the family Asteraceae, is widely distributed and mostly found in the temperate regions of North America, Asia, and Europe. Many species of *Artemisia* have significant commercial, medicinal, and economic value and are used in the traditional medicine and pharmaceutical industries [1]. Different pharmacological activities, including antimicrobial, antioxidant, anticonvulsant, anticoagulant, antidiabetic, antispasmodic, anthelmintic, cancer-fighting, cold, colic, cough, cytotoxic, cardiac stimulant, dyspepsia, fever-reducing, insecticidal, headache relief, anti-inflammatory, malaria-fighting, repellent, stomachic, and ulcer treatments have been attributed to *Artemisia* species [2]. Owing to its various therapeutic effects, this species contains various phytochemicals that have been identified and studied, including acetylenes, alkaloids, artemisolides, caffeoyl quinic acids, coumarins, flavonoids,

*Correspondence:
Sang Min Kim
kimsm@kist.re.kr
[1] Smart Farm Research Center, Korea Institute of Science and Technology (KIST) Gangneung Institute of Natural Products, Gangneung 25451, Republic of Korea
[2] Division of Bio-Medical Science & Technology, KIST School, University ofScience and Technology, Seoul 02792, Republic of Korea
[3] Natural Product Informatics Research Center, KIST Gangneung Institute of Natural Products, Gangneung 25451, Republic of Korea

polyphenolic compounds, terpenoids, sesquiterpene lactones, and sterols [3]. Since 1973, when artemisinin was obtained from *A. annua* and found to be a miracle cure for a drug-resistant strain of malaria (*Plasmodium falciparum*), other *Artemisia* species have also been grown and thoroughly studied to identify new chemical entities, particularly terpenoid constituents, that can treat a wide range of diseases [4]. Artemisinin has been used to screen other *Artemisia* species as potential new sources of agricultural output [5].

Artemisinin combination therapy is currently the most effective strategy for treating malaria and limiting its transmission [6]. It has also been proven to be effective against various parasites as well as an antiviral agent for treating hepatitis B and certain cancer cell lines. It may hold promise for combating drug-resistant cancers and exhibits potent plant-inhibiting properties, suggesting its potential as a natural herbicide [5]. Artemisinin is a sesquiterpene lactone derived from isopentenyl diphosphate that can be obtained via the mevalonate or methylerythritol phosphate pathway. Upstream, pyruvate and glyceraldehyde 3-phosphate are converted into farnesyl diphosphate [7]. The initial stage of the artemisinin biosynthetic pathway involves the modification of farnesyl diphosphate to amorpha-4,11-diene via the lyase activity of amorpha-4,11-diene synthase (ADS) (Additional file 1: Fig. S1A). The subsequent steps include the hydroxylation of artemisinic alcohol, oxidation to artemisinin aldehyde, and conversion to artemisinic acid. It is coordinated by the enzymes cytochrome P450 monooxygenase (CYP71AV1), cytochrome P450 oxidoreductase (CPR), cytochrome b5 monooxygenase (CYB5), alcohol dehydrogenase 1 (ADH1), and aldehyde dehydrogenase (ALDH1). Artemisinin aldehyde is also converted to dihydroartemisinic aldehyde by artemisinic aldehyde delta-11(13)-double-bond reductase (DBR2), which is then converted to dihydroartemisinic acid by ALDH1. Although artemisinin is formed through the photooxidation of dihydroartemisinic acid, this substrate is still considered the final enzymatically synthesized compound in the artemisinin biosynthetic pathway [8]. The pharmaceutical industry, which provides over 100 million treatments annually, is increasingly worried about the potential inability of the artemisinin supply chain to meet future demands. Although microbial based-systems capable of producing artemisinin precursors for chemical conversion have reported, agricultural production is anticipated to remain the main supply source [5].

Trichomes are hair-like organs that develop from the expansion of specialized epidermal cells, which undergo cell division, differentiation, and growth to form tissues on plant leaves or other organs. They are essential for plant taxonomy because of their variations in size, shape, morphology, quantity, and composition [9]. Trichomes play several roles in plant growth and stress tolerance. For example, barriers must be breached before any successful pathogen or herbivore attack occurs. Consequently, they are the first line of plant defense. Trichomes are typically categorized into two primary types: glandular (GTs) and non-glandular trichomes (NGTs), according to their morphology and secretory activity (Additional file 1: Fig. S1B) [10]. The fundamental morphological distinction between GTs and NGTs is the absence of a glandular head in the latter [11]. Similarly, GTs are abundant in Lamiaceae, Solanaceae, Asteraceae, and Cannabaceae, whereas NGTs are prominent in the Malvaceae and Cruciferae families of plants [7]. These two trichome types are believed to have distinct functions. NGTs typically aid in tasks such as water absorption, seed dispersal, and deterring herbivores, whereas GTs are important for the production, storage, and release of various types of secondary metabolites from plants [10]. Trichome-specific metabolites include organic acids, terpenoids, alkaloids, polysaccharides, polyphenols, and proteins. Consequently, they are an important foundation for crucial chemical compounds in the pharmaceutical, cosmetic, perfume, and food additive industries [12].

The discovery of the site of artemisinin accumulation in GTs was a significant advancement in our understanding of artemisinin biosynthesis [13]. Two distinct types of trichomes are present on the surface of *A. annua* plants. These include the GTs and T-shaped NGTs. The GTs of *A. annua* consist of ten cells: two stalk, two basal, four subapical, and two apical cells. The apical and subapical cells within the GT are responsible for the biosynthesis of artemisinin and other secondary metabolites [14]. *Artemisia* species contain a substantial amount of artemisinin, which is present in the upper cells of GTs [15]. A comparison was made between a normal biotype possessing both GTs and NGTs and a biotype containing only NGTs of *A. annua*. Artemisinin was found exclusively in the presence of GTs [13].

Artemisia, the largest genus, contains species with diverse ecology, morphology, and chemical composition [15]. Several studies have analyzed artemisinin concentrations in different species of *Artemisia*. The findings indicated that certain species within the *Artemisia* genus produce artemisinin levels comparable to those observed in *A. annua* [5]. In addition, ten different types of trichomes were identified in various species of *Artemisia,* and they included four types of GTs (capitate, peltate, pluricellular, and thin-necked) and six types of NGTs (aduncate, conical type, stinging hairy type, unicellular calavate, unicellular filiform, and unicellular tector) [12]. Capitate GTs are common in the *Artemisia* genus [15]. Among NGTs, T-shaped hairs are the most prevalent.

Furthermore, the study highlighted the significance of foliar trichomes as reliable taxonomic markers. The distinct trichome characteristics can be effectively employed to differentiate and classify different taxa within the genus *Artemisia* [16]. Notably, the density and size of GTs had no significant correlation with the artemisinin content within these species [17]. Therefore, knowledge regarding the distribution of artemisinin among *Artemisia* species is lacking, and studies on the accumulation of artemisinin and NGTs are limited.

Because of their widespread use in traditional medicine and the pharmaceutical industry, *Artemisia* species have commercial, medical, and economic significance. Artemisinin, a potent antimalarial compound that is a key metabolite in pharmaceuticals, has a beneficial relationship with GTs primarily found in *A. annua* plant leaves. Therefore, extensive studies have been conducted to investigate artemisinin in GTs. However, the coexistence of GTs and NGTs in *Artemisia* species has been observed, and the relationship between NGTs and artemisinin remains unknown. In addition, the number of GTs is not significantly associated with artemisinin levels in these species. This study evaluated the factors influencing artemisinin regulation in different *Artemisia* species by comparing artemisinin and trichome characteristics based on the species type, leaf age, and developmental stage. The ten different *Artemisia* species were collected in various ways, including young, median, and old leaves at various developmental stages (vegetative and reproductive). Subsequently, artemisinin and its derivatives, including arteannuin B, artemisinic acid, and dihydroartemisinic acid, were quantified using high-performance liquid chromatography (HPLC) analysis. Furthermore, scanning electron microscopy (SEM) images of the adaxial leaf surface were obtained to understand the micromorphological differences and measure the trichome characteristics in *Artemisia* species. To explore the factors involved in artemisinin accumulation, correlations among all parameters were analyzed using various statistical analyses, including principal component analysis (PCA) and Pearson's correlation analysis.

Materials and methods

Plant materials and chemicals

Seedlings of various *Artemisia* species were obtained from the National Institute of Horticultural and Herbal Science (Wanju, Republic of Korea) and cultivated annually in an experimental field established at the Korea Institute of Science and Technology (KIST, Gangneung, Republic of Korea) since 2019. *Artemisia* plants were exposed to outdoor conditions without any culture regulation. The descriptions of each *Artemisia* species are presented in Table 1. Samples were collected from the vegetative stage in April 2021 and the reproductive stage in October 2021. The leaves were harvested according to their age; the top three leaves were labeled as 'young,' the bottom three leaves as 'old,' and the middle leaves as 'median' (Additional file 1: Fig. S1C). The average temperature was 14.5 ℃, and the relative humidity was 59.8%, with an average precipitation of 232 mm during the harvesting period, as observed by the Korea Meteorological Administration (data.kma.go.kr). The harvested samples were stored at – 80 ℃ until further use.

Table 1 Description of different *Artemisia* species used in this study

No	Scientific name	Abbreviation
1	*Artemisia argyi*	AR
2	*Artemisia capillaris* Thunb	CA
3	*Artemisia feddei* H.Lév. & Vaniot	FE
4	*Artemisia gmelinii* Weber ex Stechm	GM
5	*Artemisia japonica* Thunb	JA
6	*Artemisia japonica* subsp. littoricola Kitam	LK
7	*Artemisia montana* Pamp	MO
8	*Artemisia princeps* Pamp	PR
9	*Artemisia princeps* Pampan. cv. sajabal	SAJ
10	*Artemisia selengensis* Turcz	SE

Analytical- and HPLC-grade solvents, including water, acetonitrile, and methanol, were purchased from Daejung (Gyeonggi, Republic of Korea). Artemisinin was purchased from Sigma-Aldrich (St. Louis, MO, USA). Arteannuin B, dihydroartemisinic acid, and artemisinic acid were purchased from ChemFace (Wuhan, Hubei, China).

HPLC analysis of artemisinin and its derivatives

Artemisia leaves were subjected to freeze-drying at – 120 ℃ for 72 h. The resulting dried material was ground to a fine powder using a mortar and pestle. A quantity of 200 mg of powder was then extracted using 10 mL of 100% methanol, which was achieved by sonication at 60 ℃ for 1 h. The upper aqueous phase was collected by centrifugation at 3000 rpm for 20 min, followed by filtration using a 0.45 μm syringe filter, and utilized for subsequent analyses.

HPLC analysis was done by using Liquid Chromatography/Mass Spectrometer at Gyeongnam Bio and Anti-aging Core Facility Center. The column used was Shiseido Capcell pak C18 (4.6 mm × 250 mm, 5 μm), and the flow rate was 1 $mL{\cdot}min^{-1}$. The oven temperature was maintained at 30 ℃, and the injection volume was 10 μL. Four compounds, artemisinin, arteannuin B, dihydroartemisinic acid, and artemisinic acid, were detected using an isocratic system with a mobile phase of acetonitrile and

water (60:40, v/v) at a detection wavelength of 197 nm. An external standard method with a calibration curve was used for quantification. In total, four artemisinin and its derivatives were used for calibration curve conduction in the range of 25 to 100 μg·mL^{-1}. The regression equations were $y = 1.2465x + 3.6005$ ($r^2 = 0.9991$), $y = 37.149x - 24.86$ ($r^2 = 0.9992$), $y = 46.676x - 45.55$ ($r^2 = 0.9996$), and $y = 38.77x - 74.38$ ($r^2 = 0.9994$) for artemisinin, arteannuin B, dihydroartemisinic acid and artemisinic acid, respectively. All measurements were conducted in triplicate.

Observation of SEM image

Freeze-dried leaf fragments cut to a tip on the outermost part of the leaves (0.5 cm) were prepared for SEM analysis. The adaxial surfaces of the leaves were fixed to a specimen holder using carbon tape. The specimens were sputter-coated with gold–palladium for 1–2 min using a Leica EM SCD005 microscope (Leica Microsystems). The coated specimens were moved to the chamber and analyzed under a field-emission scanning electron microscope (FE-SEM, Inspect F, ELECMI, Madrid, Spain). The electron beam was set at 10 kV, and the central portion of the specimen was captured as an image. To compare the distribution of *Artemisia* species depending on the developmental stage and leaf age, the positions of each GT and NGT were marked and counted using appropriately magnified SEM images. To observe the size of the GTs, the major (A) and minor (B) axes of the ellipse were measured and calculated using the following formula [18]:

$$\text{Size of GT } (\mu\text{m2}) = \frac{AB\pi}{4}$$

To determine the size of the GTs, we randomly selected three and observed the axes from one leaf fragment. The average value was calculated and used as the representative value for each replicate. All measurements were performed using an ImageJ analyzer and carried out with three biological replicates.

PCA and Pearson's correlation analysis

The PCA was performed using the statistical software package SPSS 26.0 (SPSS Inc., Chicago, IL, USA). In the biplot, each point symbolizes a different sample, and distinct colors indicate individual groups. The arrows reflect the original variables, and their directions display correlations between the original and principal components. Additionally, loading plots of the four quantified compounds and trichome characteristics from *Artemisia* species were obtained using MetaboAnalyst 5.0 with auto-scaling (https://www.metaboanalyst.ca/). Pearson's correlation coefficient was applied to a series of measurements of artemisinin and its derivative contents paired with trichome characteristics. The range of the sample correlation coefficient was between -1 and 1, and p-value < 0.05 was considered statistically significant. A color scheme from red (negative correlation, ranging from -1 to 0) to blue (positive correlation, ranging from 0 to 1) and white (no correlation) was used to display the coefficient of correlation for each factor. The biplot, correlation coefficient plot, and Pearson correlation coefficient scatter plot were visualized using SRplot (https://www.bioinformatics.com.cn/en), a free online platform for data analysis and visualization.

Statistical analysis

All statistical analyses were performed using the statistical software package SPSS 26.0 (SPSS Inc., Chicago, IL, USA). We performed a t-test to compare the differences in artemisinin and total artemisinin derivative content according to developmental stages in the same *Artemisia* species. A one-way analysis of variance (ANOVA) was conducted to assess significant differences based on the type of species at the same developmental stage using Duncan's multiple range test at the $p < 0.05$ significance level. A three-way ANOVA was performed to assess significant differences in the effects of *Artemisia* species, developmental stage, and leaf age on each tested factor. All measurements were observed from three biological replicates and presented as the mean ± standard deviation.

Results

Distribution differences of artemisinin and its derivatives based on developmental stages and leaf age in different *Artemisia* species

Artemisinin and its derivatives, including arteannuin B, artemisinic acid, and dihydroartemisinic acid, were analyzed in different *Artemisia* species based on their developmental stage and leaf age. Among the four artemisinin derivatives, artemisinin was predominant in most *Artemisia* species (Additional file 1: Fig. S2). For example, in the case of PR, where all compounds were identified, artemisinin was abundant at 5.49 mg·g^{-1} dry weight (DW), followed by arteannuin B at 0.41 mg·g^{-1} DW, artemisinic acid at 0.18 mg·g^{-1} DW, and dihydroartemisinic acid at 0.03 mg·g^{-1} DW (Fig. 1A). Owing to the abundance of artemisinin as a major compound in this species, the variation in artemisinin at different developmental stages among various *Artemisia* species is depicted (Fig. 1B). During the vegetative stage, artemisinin was most significantly accumulated in the CA leaves, with a concentration of 24.7 mg·g^{-1} DW. In addition, AR, PR, and SAJ belonged to the high group of artemisinin with concentrations of 11.3, 5.5, and 6.4 mg·g^{-1} DW, respectively. However, in other *Artemisia* species,

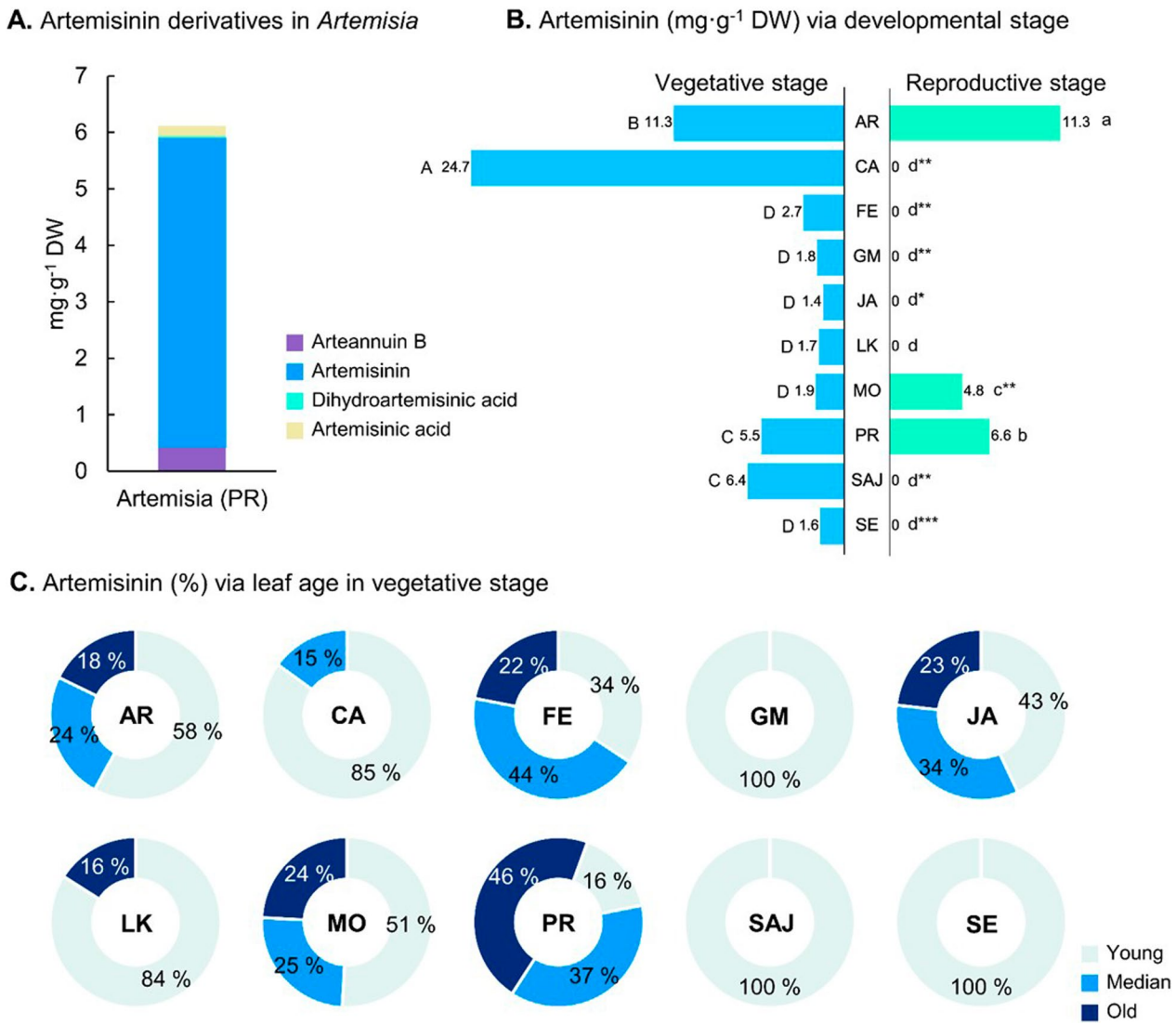

Fig. 1 **A** Representative distribution of artemisinin and its derivatives in *Artemisia* species. The data in the bar graph was observed from PR in the vegetative stage. **B** Distribution of artemisinin based on the developmental stages. The value next to each bar represents each artemisinin content (mg·g^{-1} DW). Upper and lowercase letters represent significant differences in artemisinin content between *Artemisia* species in the vegetative and reproductive stages, respectively, by one-way ANOVA ($p < 0.05$). The asterisks indicate significant differences between developmental stages in the same species by t-test (*, $p < 0.05$; **, $p < 0.01$; ***, $p < 0.001$). **C** Distribution of artemisinin based on leaf age from different *Artemisia* species in the vegetative stage. The values shown in the donut chart reveal the percentage of each content obtained according to leaf age by total artemisinin content

the artemisinin content was distributed at relatively low concentrations, ranging from 1.4 to 2.7 mg·g^{-1} DW. During the reproductive stage, artemisinin was not detected in the leaves of most *Artemisia* species, except for AR, MO, and PR. This indicates that artemisinin decreases as the developmental stage progresses from the vegetative to the reproductive stages. Notably, in AR and PR, the artemisinin content remained relatively consistent; conversely, the artemisinin content increased in MO during the developmental stage progression.

The distribution of the relative ratio of artemisinin content from each *Artemisia* species based on leaf age during different developmental stages was also analyzed by conversion into a percentage relative to the total artemisinin content of the leaves. Notable differences were observed in the levels of this compound regarding leaf age among the species. Specifically, artemisinin predominantly accumulated in young leaves of most species during the vegetative stage (Fig. 1C). However, a similar distribution of its content was observed across all leaves in FE, and there

was an increase as leaf age progressed, in the opposite direction to that of PR. The relative ratio of artemisinin content based on leaf age during the reproductive stage for artemisinin-positive *Artemisia* species, including AR, MO, and PR, is shown (Additional file 1: Fig. S3). In these species, artemisinin was predominantly produced in young leaves. In the case of MO, where the artemisinin content increased as the developmental stage progressed, the accumulated artemisinin in young leaves contributed significantly.

The results of the analysis of artemisinin and its derivatives from different *Artemisia* species based on developmental stage and leaf age are presented in Additional file 1: Table S1. The three artemisinin derivatives did not significantly accumulate in this species compared to artemisinin itself. Furthermore, they followed a similar trend to the artemisinin content, with a decrease or minimal accumulation as the developmental stages transitioned from vegetative to reproductive. For example, arteannuin B was not detected in most *Artemisia* species as the developmental stage progressed, except in SE, where it increased slightly. *Artemisia* species (FE, JA, LK, MO, and PR) containing artemisinic acid were not detected during the vegetative stage. Similarly, dihydroartemisinic acid was only detected in the young leaves of AR and PR during the reproductive stage and exhibited a decreasing pattern in most species during the transition from the vegetative to the reproductive stage. Based on leaf age, artemisinin derivatives showed distinct distribution patterns across different *Artemisia* species. Most *Artemisia* species in which arteannuin B was detected showed a decreasing trend in content as leaf age progressed during the vegetative stage, except for FE, which showed a similar content, and LK, which increased. Similar to other artemisinin derivatives, FE, LK, and PR for artemisinic acid accumulated the most in young leaves and decreased as the leaves grew older. Different patterns were observed among the various *Artemisia* species depending on leaf age. For example, artemisinic acid in JA and MO and dihydroartemisinic acid in AR and PR increased from young to medium leaves and decreased in old leaves during the vegetative stage. Therefore, our study indicates that artemisinin biosynthesis may vary depending on species, developmental stage, and leaf age.

Morphological observation and density of trichomes in the different *Artemisia* species

Photographs of leaf shapes and SEM images of the adaxial leaf surfaces of young, median, and old leaves from different *Artemisia* species are shown (Fig. 2). The leaf morphology of the different *Artemisia* species varied, and SEM images revealed differences in trichome distribution according to species type and leaf age. Various types of trichomes have also been identified in *Artemisia* species, such as NGTs acquired from AR and GM. According to presence and absence of glandular head, we classified GTs and NGTs among *Artemisia* species in this study. Furthermore, we separately counted each trichome to observe trichome density and measured the size of GTs based on the developmental stage and leaf age in different *Artemisia* species.

A distinct difference in the density of GTs and NGTs among *Artemisia* species was evident (Fig. 3 and Additional file 1: Table S2). For example, species AR and SAJ exhibited high trichome densities in both GTs and NGTs, whereas species SE, JA, and LK had very few trichomes of both types. Additionally, there were species such as CA, MO, and PR with a low density of GTs but a high density of NGTs. Examination of the changes in trichome density according to developmental stage revealed that the GT density in the most of *Artemisia* species such as AR, FE, GM, JA, PR, SAJ increased as they progressed from the vegetative to reproductive stages. Conversely, as the developmental stages transitioned, NGT density decreased in most *Artemisia* species, including CA, FE, GM, LK, MO, PR, and SAJ. During the vegetative stage, GT density increased from young to median leaf age, followed by a decrease from median to old leaf age in most cases. However, it generally decreased from young to old leaves during the reproductive stage. Regardless of the developmental stage, NGT density consistently decreased from young to old leaves.

Artemisinin typically accumulates in the GTs of *A. annua*, and the size of the GT may affect the accumulation of bioactive compounds. In this study, we measured the size of GTs based on *Artemisia* species, developmental stages, and leaf age (Additional file 1: Fig. S4 and Table S2). We observed that GT size increased as leaf age progressed from young to old leaves. Additionally, during the transition from the vegetative to the reproductive stage, the GT size on young leaves was larger than that in the vegetative stage. This suggests that after vegetative growth ceases, the size of the trichomes on young leaves gradually increases as reproductive growth progresses.

Correlation analysis between artemisinin derivative contents and trichome characteristics

PCA, also known as unsupervised multivariate analysis, is used to detect differences both inside and between groups of samples [19]. In this study, we applied PCA to differentiate and cluster the developmental stage, leaf age, and species in *Artemisia* plants according to their artemisinin derivatives contents and trichome characteristics as the explanatory variables. The percentages, cumulative values, and eigenvalues of the principal components are presented (Table 2). Based

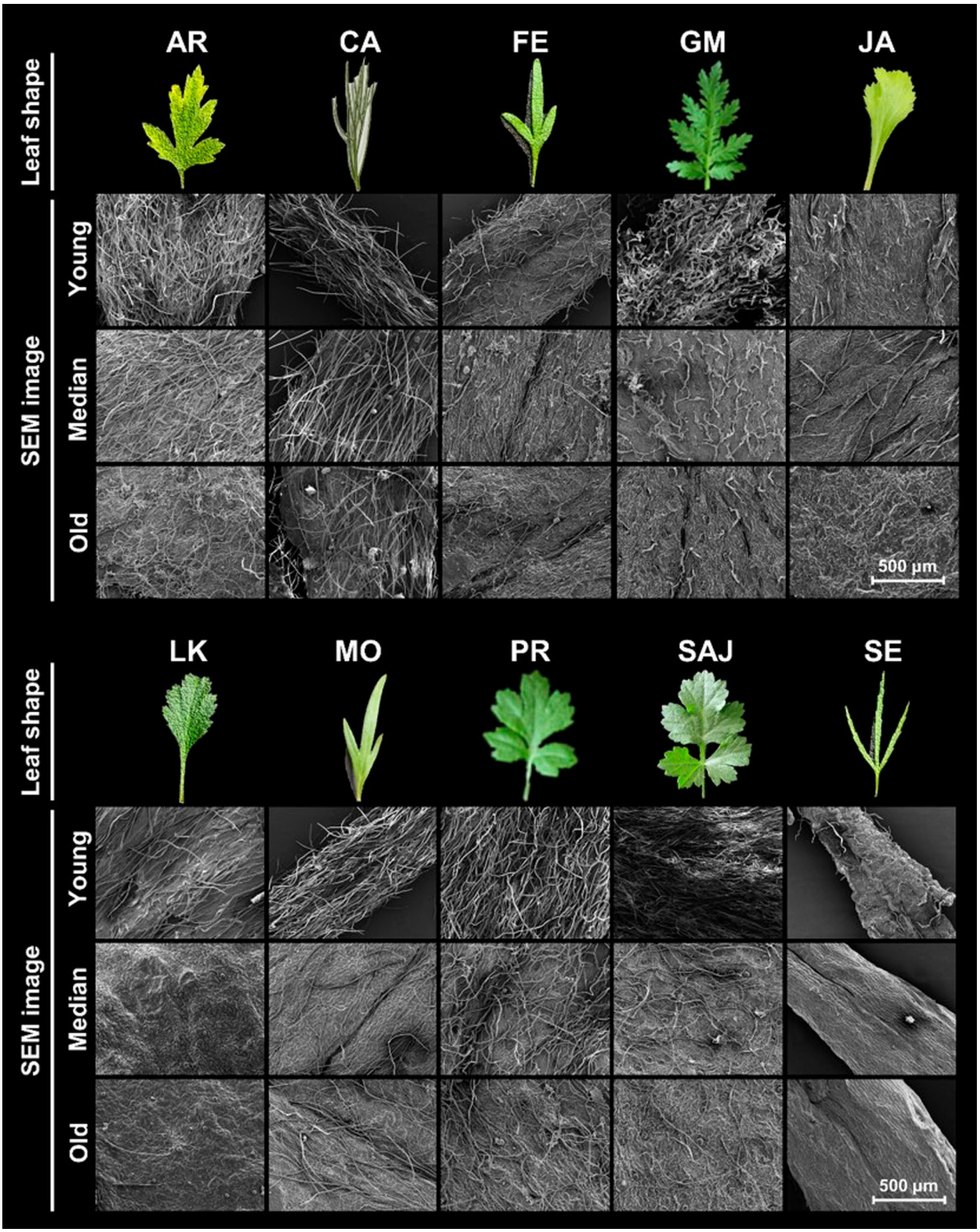

Fig. 2 Representative photographs of leaf shape and SEM of the young, median, and old adaxial leaf surface obtained from different *Artemisia* species

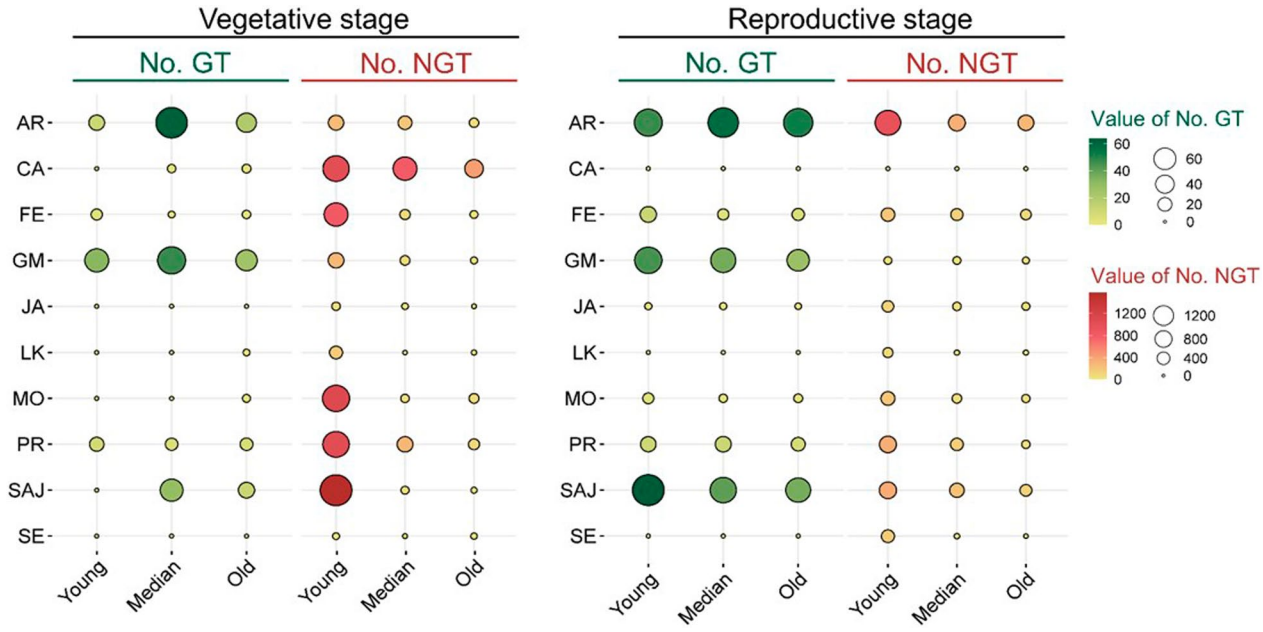

Fig. 3 Bubble chart depicting GT and NGT density changes based on developmental stage and leaf age. Each bubble represents the number of trichomes (per 1 mm^2) on the adaxial leaf surface from different *Artemisia* species. The color of the bubbles indicates the range from the group with a low number of each trichome (yellow) to the group with a high number (green for GT and red for NGT). No. GT, number of glandular trichomes; No. NGT, number of non-glandular trichomes

Table 2 Eigenvalue, percentage variation, and cumulative variance derived from PCA

	PC1	PC2	PC3	PC4	PC5	PC6	PC7
Eigenvalue	2.026	1.769	0.983	0.802	0.611	0.445	0.364
Percentage of variance (%)	28.95	25.27	14.05	11.46	8.72	6.35	5.20
Cumulative variance (%)	28.95	54.22	68.26	79.73	88.45	94.80	100.00

on the first two PCA components, the principal components (PC1 and PC2) accounted for 54.2% of the total variance (Fig. 4). PC1 explained 28.9% of the variance, while PC2 explained 25.3%. The biplots (upper panel in Fig. 4) represent the scores of explanatory variables as vectors (black arrow, $n=7$) and the individuals of each group (colored circles). The black arrow extending from the central point of the PCA biplot represents the positive or negative correlations of various variables, and their proximity indicates the correlation strength. In the biplot analysis, they were not distinctly separated based on the developmental stage (Fig. 4A), leaf age (Fig. 4B), or *Artemisia* species (Fig. 4C) because of their poor correlation. However, notably, artemisinin content was positively correlated with the number of NGTs in PC1 observed from all biplots. The loading plots (lower panel in Fig. 4) indicated the relationship between the examined traits and how they contributed to discrimination. Similarly, artemisinin and the NGTs were positioned close to each other in the loading plots.

Pearson's correlation analysis was applied to the artemisinin derivative content and trichome characteristics to support these findings. We represented the correlation coefficients between all factors as a correlation matrix (Fig. 5A). In the correlation analysis of the artemisinin derivatives, artemisinin showed a correlation coefficient of 1 ($p<0.0001$) with the total compounds obtained from the sum of all artemisinin derivative contents, indicating a strong positive correlation (Additional file 1: Table S3). However, no significant correlations were observed between artemisinin and the other derivatives. Furthermore, no correlation was found between the artemisinin derivatives and artemisinin derivatives or total compounds. The number and size of GTs were positively correlated (correlation coefficient = 0.52; $p<0.0001$) with trichome characteristics; however, NGTs did not show

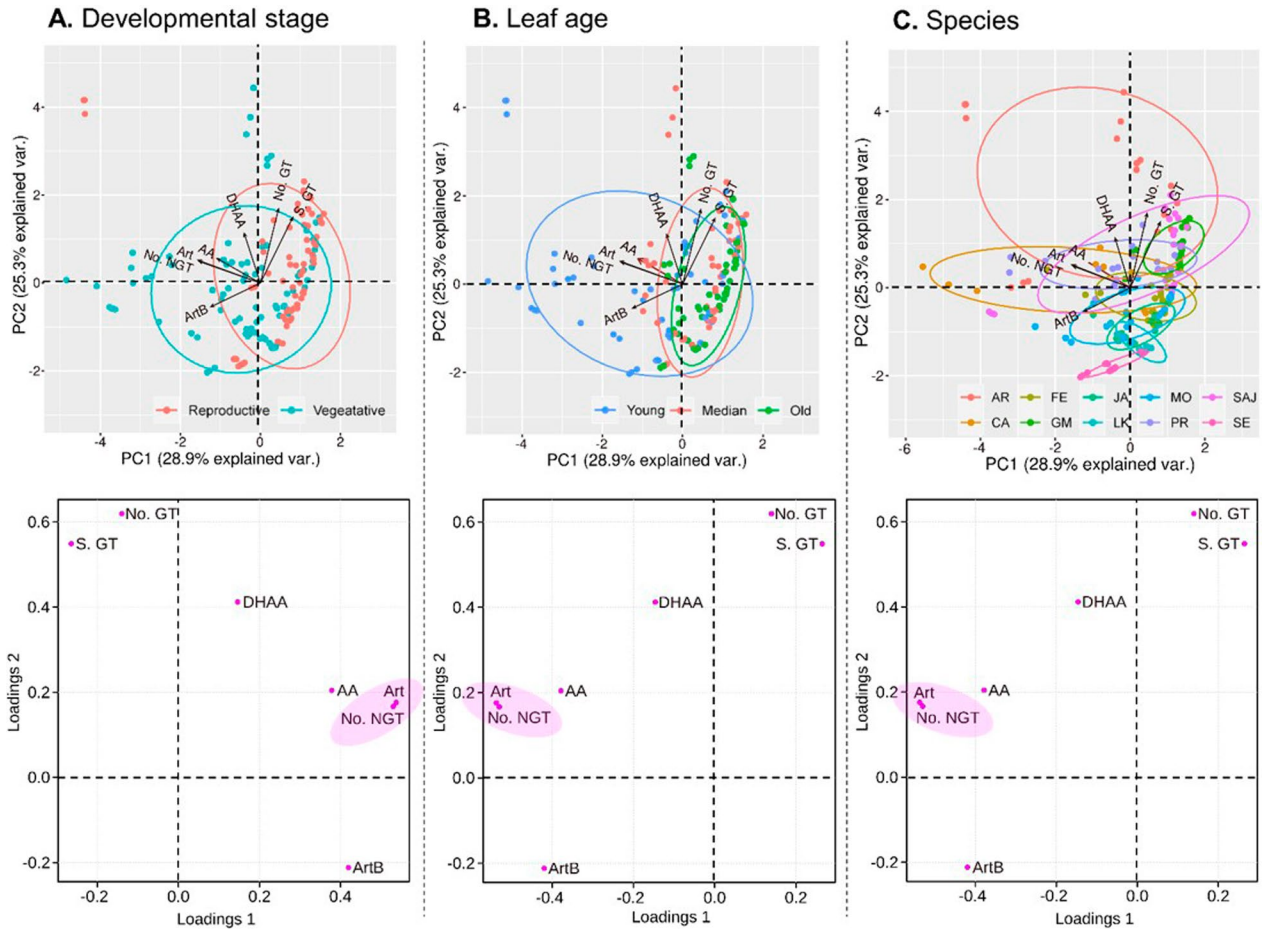

Fig. 4 Biplot (upper) and loading plot (lower) obtained using PCA based on **A** developmental stage, **B** leaf age, and **C** species in *Artemisia* plants. The explanatory variables included artemisinin (Art), arteannuin B (ArtB), dihydroartemisinic acid (DHAA), artemisinic acid (AA), the number of GTs (No. GT), the number of NGTs (No. NGT), and size of GTs (S. GT)

any significant correlation. Notably, the artemisinin content and the number of NGTs had a positive correlation coefficient of 0.56 ($p < 0.0001$) (Fig. 5B). In contrast, artemisinin did not correlate with the number or size of GTs, with correlation coefficients of -0.011 ($p = 0.88$) and -0.075 ($p = 0.33$), respectively (Fig. 5C and 5D). Based on these findings, it has been suggested that the number of NGTs, rather than the number and size of GTs, positively correlates with artemisinin and certain derivative content in *Artemisia* species.

Discussion

Distribution of artemisinin and its derivatives content in species, developmental stage, and leaf age

This study examined artemisinin and its derivatives, arteannuin B, artemisinic acid, and dihydroartemisinic acid, in distinct *Artemisia* species by considering developmental stages and leaf age as factors (Additional file 1: Table S4). As observed from the strong positive correlation between the total compound content and the artemisinin content, artemisinin accumulated prominently among the four analyzed compounds in all *Artemisia* species (Fig. 1A and Additional file 1: Fig. S2). Furthermore, artemisinin content varied widely among different *Artemisia* species in the vegetative stage, ranging from 1.4 to 24.7 $mg{\cdot}g^{-1}$ DW (Fig. 1B). Previous studies have also investigated the variations in the distribution of artemisinin content among *Artemisia* species, which is consistent with our findings. An analysis of artemisinin content from 16 *Artemisia* species at the vegetative stage found that *A. annua* had the highest content, with 5.65 $mg{\cdot}g^{-1}$ DW. However, there were also species, such as *A. khorassanica,* in which artemisinin was not detected [20]. Furthermore, artemisinin was mostly deposited in young leaves, with a declining tendency as leaf age advanced from young to old (Fig. 1C). This is consistent with earlier studies showing that senescent leaves contain nearly half of the total artemisinin

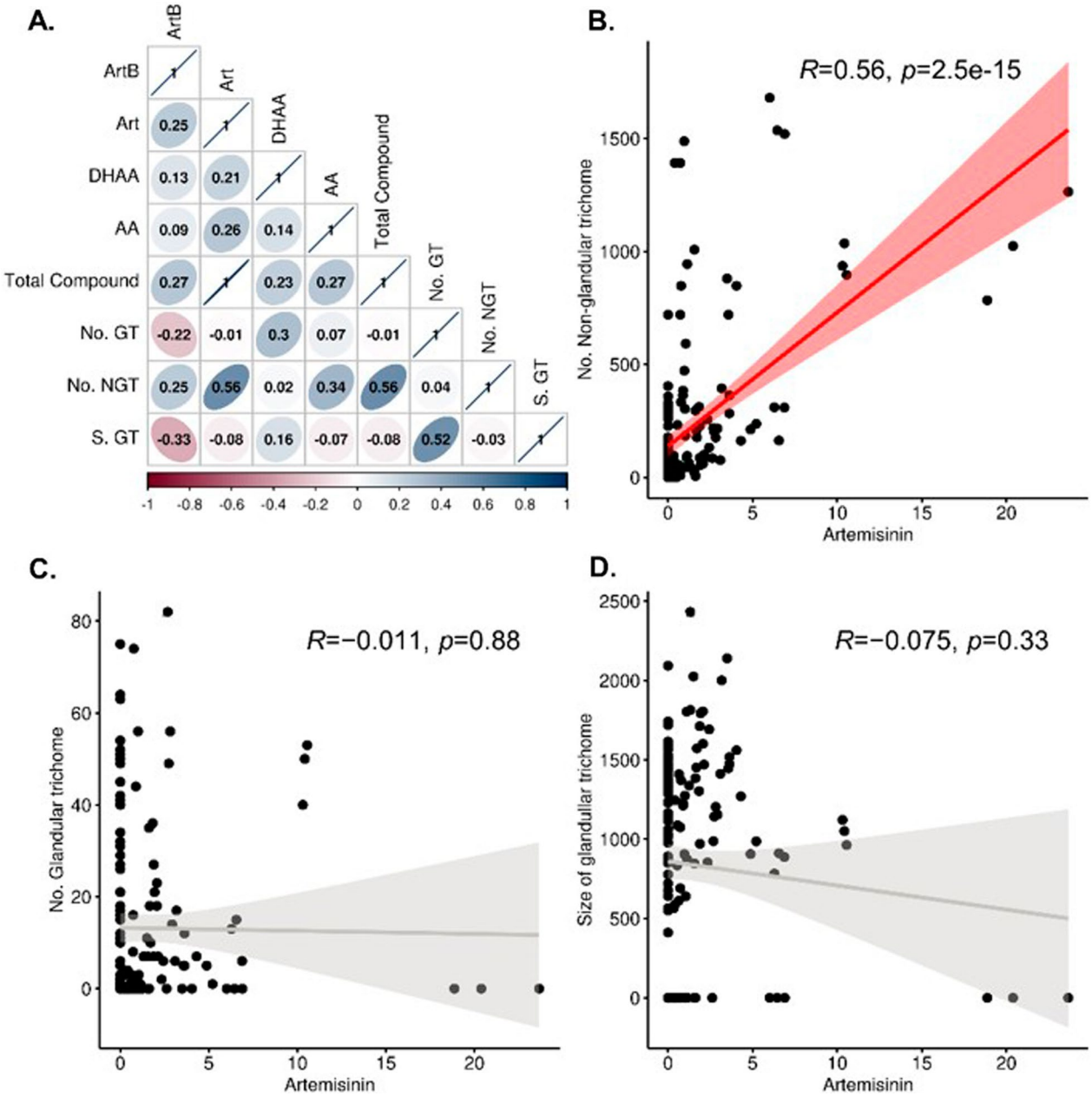

Fig. 5 **A** Correlation matrix showing the results of Pearson's correlation analysis. Pearson correlation coefficient values and directions are marked with different colors: positive correlation (from white to blue on the color scale) and negative correlation (from white to red). Scatter plot of Pearson's correlation coefficient between artemisinin content and **B** the number of NGTs, **C** the number of GTs, and **D** the size of GTs in *Artemisia* species, respectively. AA, artemisinic acid, Art, artemisinin, ArtB, arteannuin B, DHAA, dihydroxyartemisinic acid, No. GT, number of glandular trichomes; No. NGT, number of non-glandular trichomes; S. GT, size of GT

in mature plants of *A. annua* [21]. The levels of certain precursors, including artemisinic and dihydroartemisinic acids, which are frequently several orders of magnitude higher than those of artemisinin, appear to change with respect to environmental, genetic, and epigenetic factors [22].

Consistent with earlier studies on other *Artemisia* species, the artemisinin content in *Artemisia* leaf tissue primarily decreased as the growth stage changed from vegetative to reproductive. The artemisinin content and the expression levels of genes involved in its biosynthetic pathway have been investigated at different developmental stages, including vegetative, budding, and flowering.

Accordingly, some species, including *A. absinthium*, *A. diffusa*, *A. sieberi*, and *A. spicigeria,* exhibited the highest levels of artemisinin production in their flowers during flowering. In contrast, other species, such as *A. annua*, *A, campestris*, and *A. vulgaris,* reached peak artemisinin production in the buds during the budding stage. Notably, *A. scoparia* was the only species with the highest artemisinin content in its leaves during the vegetative stage [23]. It can be inferred that artemisinin accumulation occurs in reproductive tissues such as flowers and buds in most *Artemisia* species as the growth stage progresses from the vegetative to the reproductive stage.

Artemisinin exhibited distinct differences in its accumulation pattern regarding leaf age among different species. In most *Artemisia* species, artemisinin primarily accumulated in young leaves, and there was a decreasing trend as the leaves age. This is consistent with previous studies showing that younger leaves exhibit greater trichome development and produce more artemisinin than older leaves [24]. A notable finding in mature plants was that senescent leaves contribute approximately half of the total artemisinin content within the *A. annua* plant [21]. However, there was a different pattern, with increased artemisinin content as leaf age progressed or a similar distribution across all leaves. Therefore, these findings show the variability in artemisinin accumulation regarding leaf age among the different *Artemisia* species in this study.

Trichome development based on plant growth stage and leaf age

Significant features for identifying species can be found in the epidermis of the leaves. Some of these characteristics are the distribution and orientation of stomata, size of guard cells, number of subsidiary cells, and types of specific GTs and NGTs [15]. Several trichome types, such as 10-celled biseriate GTs and T-shaped NGTs, have been reported in various *Artemisia* species [25]. The qualitative and quantitative characteristics of all trichomes were observed in the 13 *Artemisia* species. Morphological features, such as the presence or absence of certain trichomes, can be used to distinguish various species within the genus *Artemisia* [12]. This is consistent with our finding that there was an apparent difference in the distribution of GTs and NGTs among *Artemisia* species (Additional file 1: Table S5). For example, some species, such as AR, had abundant GTs and NGTs, whereas others, such as SE, were scarce (Fig. 3). Furthermore, morphological variations were observed in the NGTs (Fig. 2). The AR and GM display several forms of NGTs. AR had a sharp, stinging hair trichome with a sting-like apex, similar to the findings of a previous study. Unlike the AR, the GM had an aduncate-type NGT that was long and had a curled or hook-like apex [12].

Trichome density is also known to be affected by developmental factors such as plant and leaf age. The formation of abaxial trichomes on *Arabidopsis* leaf blades is used as a morphological marker of vegetative phase change [26]. Our findings showed that when most *Artemisia* species developed from the vegetative to reproductive stages, the density of their GTs increased; however, the density of NGTs decreased. Similarly, the density of type IV trichome (GT, with a short multicellular stalk and a small gradient at the tip) changed with maturity in *Solanum pimpinellifolium*. Trichome density increased, reaching the maximum median as the plants grew older [27]. The GT density decreased from young to old leaves (Fig. 3). Consistently, younger leaves develop more GTs and produce more artemisinin than older leaves in *A. annua* [28]. In addition, the influence of leaf age on the type IV trichomes of *S. pimpinellifolium* was determined. This finding demonstrated that the number of trichomes in young leaves decreased as the leaflets expanded in the second and third leaves [27].

Correlation between artemisinin and trichome in different *Artemisia* species

As GTs were discovered to be the sole site of artemisinin biosynthesis, almost all knowledge about artemisinin biosynthesis has come from studies on GTs, which are secretory cells with specialized metabolism that emit volatiles. GTs have been the sole focus of artemisinin research over the past two decades [29, 30]. Studies have also identified a majority of genes and transcription factors in GTs, and many studies have shown the significance of GT cells in the regulation of artemisinin biosynthesis [30]. Artemisinin biosynthesis was previously considered to be specific to *A. annua*; however, recent studies have revealed that artemisinin exists in other *Artemisia* species. Eight *Artemisia* species were selected and examined to determine the levels of artemisinin biosynthetic genes at the three distinct developmental stages. Among the different species, the only species with the highest artemisinin content at the vegetative stage was *A. scoparia*, which was correlated with high GT density in the leaf tissue. They also suggested that the competition between ADS and other sesquiterpene synthases using farnesyl diphosphate as a substrate may depend on the species [23]. Subsequently, this study evaluated the leaves of five *Artemisia* species with varying artemisinin contents with respect to GT density, as well as the expression of artemisinin biosynthetic genes and trichome formation-related genes. Accordingly, neither GT density ($R^2 = 0.024$ ns) nor size ($R^2 = 0.010$ ns) was significantly correlated with artemisinin within these species [20]. As

GTs are the site of artemisinin synthesis, more trichomes should increase artemisinin accumulation. However, this theory is yet to be proven in *Artemisia* species.

Our findings suggest that the number of NGTs, as opposed to the number and size of GTs, positively correlated with artemisinin (R = 0.56). The correlation coefficient, normally abbreviated as R, denotes the direction and strength of the correlation between two variables [31]. A correlation of 0.56 indicated a moderately positive correlation based on a rule-of-thumb scale to evaluate the correlation coefficient [32]. The novelty of this study is that, for the first time, the density of NGTs may influence artemisinin content among *Artemisia* species. For example, in the vegetative stage of CA, there were 1,024 NGT on young leaves, with a notable accumulation of artemisinin at 20.97 $mg{\cdot}g^{-1}$ DW. Likewise, in the vegetative stage of SAJ, there were 1,579 NGT on young leaves, and the artemisinin content was 6.45 $mg{\cdot}g^{-1}$ DW (Additional file 1: Tables S1 and S2). These findings suggest that these species likely contributed to the correlation results obtained. Studies on artemisinin biosynthesis in the NGTs of these species are limited. Differential transcriptome analysis of GTs and NGTs (T-shaped with stalks and elongated cells) has been reported in *A. annua* [33]. Notably, the potential mechanisms associated with artemisinin biosynthesis in NGT cells have been suggested for *A. annua*. This study showed that NGT cells obtained from self-pollinated inbred *A. annua* plants expressed artemisinin biosynthetic genes. GT-free leaves and cells also produced artemisinin and its derivatives. Subsequently, the leaves of *A. annua glandless* mutants biosynthesized artemisinin [34]. This finding supports our results. Collectively, these findings may accelerate the development of novel strategies for achieving high and constant artemisinin production.

In the present study, an intricate relationship between artemisinin and its derivatives, trichome characteristics, and various factors such as species type, developmental stage, and leaf age was demonstrated in *Artemisia* species. Our findings revealed that artemisinin and its derivatives displayed diverse distribution patterns that were influenced by species and leaf age, with a declining trend as the developmental stage progressed. This highlights the complexities of artemisinin regulation and accumulation in *Artemisia* species. Differences in leaf shape, trichome morphology, and trichome distribution were also observed. The distinctive characteristics observed among different *Artemisia* species further emphasize the complex interactions between these factors. Though they did not clearly divide into groups by type of species, developmental stage, and species, PCA unveiled a positive relationship between artemisinin and the number of NGTs, with a correlation coefficient of 0.56 ($p < 0.0001$). Therefore, this research advances our understanding of the factors affecting artemisinin levels in *Artemisia* species as well as highlights the need for future investigations into the specific functions of NGTs in artemisinin biosynthesis. Furthermore, through an overall comparison of artemisinin content, we determined the potential for substitutes like *A. annua* to replace supply species, such as CA and AR.

Abbreviations

DW	Dry weight
GT	Glandular trichome
HPLC	High-performance liquid chromatography
NGT	Non-glandular trichome
PCA	Principal component analysis
SEM	Scanning electron microscope

Supplementary Information

The online version contains supplementary material available at https://doi.org/10.1186/s13765-024-00883-w.

Additional file 1. Tables and Figures.

Author contributions

YJP conceptualized and performed the experiments, visualized the data, and prepared and edited the original manuscript. TQT conducted sample collection and edited the manuscript. YBC, PKH, JM, and SYK contributed to data interpretation and edited the manuscript. HSK provided the study materials. SMK conceptualized and supervised the research, edited the manuscript, and contributed to the funding acquisition.

Funding

This work was supported by the Korea Institute of Planning and Evaluation for Technology in Food, Agriculture and Forestry (IPET) and Korea Smart Farm R&D Foundation (KosFarm) through the Smart Farm Innovation Technology Development Program, funded by Ministry of Agriculture, Food and Rural Affairs (MAFRA), Ministry of Science and ICT (MSIT), and Rural Development Administration (RDA) (421034-04).

Availability of data and materials

The datasets used and/or analysed during the current study are available from the corresponding author on reasonable request.

Competing interests

The authors declare that they have no competing interests.

Received: 12 December 2023 Accepted: 3 March 2024
Published online: 21 March 2024

References

1. Singh P, Bajpai V, Khandelwal N, Varshney S, Gaikwad AN, Srivastava M, Singh B, Kumar B (2021) Determination of bioactive compounds of *Artemisia* Spp. plant extracts by LC-MS/MS technique and their in-vitro anti-adipogenic activity screening. J Pharm Biomed Anal 193:113707
2. da Silva JAT, Yonekura L, Kaganda J, Mookdasanit J, Nhut DT, Afach G (2005) Important secondary metabolites and essential oils of species within the Anthemideae (Asteraceae). J Herbs Spices Med Plants 11:1–46
3. Bora KS, Sharma A (2011) The genus *Artemisia*: a comprehensive review. Pharm Biol 49:101–109
4. Brown GD (2010) The biosynthesis of artemisinin (Qinghaosu) and the phytochemistry of *Artemisia annua* L. (Qinghao). Molecules 15:7603–7698

5. Mannan A, Ahmed I, Arshad W, Asim MF, Qureshi RA, Hussain I, Mirza B (2010) Survey of artemisinin production by diverse *Artemisia* species in northern Pakistan. Malar J 9:1–9
6. Mutabingwa TK (2005) Artemisinin-based combination therapies (ACTs): best hope for malaria treatment but inaccessible to the needy! Acta Trop 95:305–315
7. Xiao L, Tan H, Zhang L (2016) *Artemisia annua* glandular secretory trichomes: the biofactory of antimalarial agent artemisinin. Sci Bull 61:26–36
8. Hassani D, Fu X, Shen Q, Khalid M, Rose JK, Tang K (2020) Parallel transcriptional regulation of artemisinin and flavonoid biosynthesis. Trends Plant Sci 25:466–476
9. Schilmiller AL, Last RL, Pichersky E (2008) Harnessing plant trichome biochemistry for the production of useful compounds. Plant J 54:702–711
10. Wu T, Wang Y, Guo D (2012) Investigation of glandular trichome proteins in *Artemisia annua* L. using comparative proteomics. PLoS ONE 7:41822
11. Werker E (2000) Trichome diversity and development. Adv Bot Res 31:1–35
12. Hussain A, Hayat MQ, Sahreen S, Bokhari SAI (2019) Unveiling the foliar epidermal anatomical characteristics of genus *Artemisia* (Asteraceae) from northeast (Gilgit-Baltistan), Pakistan. Int J Agric Biol 21:630–638
13. Duke MV, Paul RN, Elsohly HN, Sturtz G, Duke SO (1994) Localization of artemisinin and artemisitene in foliar tissues of glanded and glandless biotypes of *Artemisia annua* L. Int J Plant Sci 155:365–372
14. Soni R, Shankar G, Mukhopadhyay P, Gupta V (2022) A concise review on *Artemisia annua* L.: A major source of diverse medicinal compounds. Ind Crops Prod 184:115072
15. Hussain A (2020) The genus *Artemisia* (Asteraceae): A review on its ethnomedicinal prominence and taxonomy with emphasis on foliar anatomy, morphology, and molecular phylogeny. Proc Pak Acad Sci 57:1–28
16. Hayat MQ, Ashraf M, Khan MA, Yasmin G, Shaheen N, Jabeen S (2009) Diversity of foliar trichomes and their systematic implications in the genus *Artemisia* (Asteraceae). Int J Agric Biol 11:566–570
17. Salehi M, Karimzadeh G, Naghavi MR, Naghdi Badi H, Rashidi Monfared S (2018) Expression of key genes affecting artemisinin content in five *Artemisia* species. Sci Rep 8:12659
18. Maes L, Van Nieuwerburgh FC, Zhang Y, Reed DW, Pollier J, Vande Casteele SR, Inzé D, Covello PS, Deforce DL, Goossens A (2011) Dissection of the phytohormonal regulation of trichome formation and biosynthesis of the antimalarial compound artemisinin in *Artemisia annua* plants. New Phytol 189:176–189
19. Liu C, Liu S, Tse WM, Tse KWG, Erbu A, Xiong H, Lanzi G, Liu Y, Ye B (2023) A distinction between *Fritillaria Cirrhosa* Bulbus and *Fritillaria Pallidiflora* Bulbus via LC–MS/MS in conjunction with principal component analysis and hierarchical cluster analysis. Sci Rep 13:2735
20. Salehi M, Karimzadeh G, Naghavi MR, Badi HN, Monfared SR (2018) Expression of artemisinin biosynthesis and trichome formation genes in five *Artemisia* species. Ind Crops Prod 112:130–140
21. Lommen WJ, Elzinga S, Verstappen FW, Bouwmeester HJ (2007) Artemisinin and sesquiterpene precursors in dead and green leaves of *Artemisia annua* L. crops. Planta Med 73:1133–1139
22. Arsenault PR, Wobbe KK, Weathers PJ (2008) Recent advances in artemisinin production through heterologous expression. Curr Med Chem 15:2886–2896
23. Ranjbar M, Naghavi MR, Alizadeh H, Soltanloo H (2015) Expression of artemisinin biosynthesis genes in eight *Artemisia* species at three developmental stages. Ind Crops Prod 76:836–843
24. Nguyen KT, Arsenault PR, Weathers PJ (2011) Trichomes + roots + ROS = artemisinin: regulating artemisinin biosynthesis in *Artemisia annua* L. In Vitro Cell Dev Biol Plant 47:329–338
25. Ferreira JF, Janick J (1995) Floral morphology of *Artemisia annua* with special reference to trichomes. Int J Plant Sci 156:807–815
26. Telfer A, Bollman KM, Poethig RS (1997) Phase change and the regulation of trichome distribution in *Arabidopsis thaliana*. Development 124:645–654
27. Mata-Nicolás E, Montero-Pau J, Gimeno-Paez E, García-Pérez A, Ziarsolo P, Blanca J, Van der Knaap E, Díez MJ, Cañizares J (2021) Discovery of a major QTL controlling trichome IV density in tomato using K-seq genotyping. Genes 12:243
28. Arsenault PR, Vail D, Wobbe KK, Erickson K, Weathers PJ (2010) Reproductive development modulates gene expression and metabolite levels with possible feedback inhibition of artemisinin in *Artemisia annua*. Plant Physiol 154:958–968
29. Tellez MR, Canel C, Rimando AM, Duke SO (1999) Differential accumulation of isoprenoids in glanded and glandless *Artemisia annua* L. Phytochemisty 52:1035–1040
30. Chen M, Yan T, Shen Q, Lu X, Pan Q, Huang Y, Tang Y, Fu X, Liu M, Jiang W (2017) GLANDULAR TRICHOME-SPECIFIC WRKY 1 promotes artemisinin biosynthesis in *Artemisia annua*. New Phytol 214:304–316
31. Mukaka MM (2012) A guide to appropriate use of correlation coefficient in medical research. Malawi Med J 24:69–71
32. Asuero AG, Sayago A, González A (2006) The correlation coefficient: An overview. Crit Rev Anal Chem 36:41–59
33. Soetaert SS, Van Neste CM, Vandewoestyne ML, Head SR, Goossens A, Van Nieuwerburgh FC, Deforce DL (2013) Differential transcriptome analysis of glandular and filamentous trichomes in *Artemisia annua*. BMC Plant Biol 13:1–14
34. Judd R, Bagley MC, Li M, Zhu Y, Lei C, Yuzuak S, Ekelöf M, Pu G, Zhao X, Muddiman DC (2019) Artemisinin biosynthesis in non-glandular trichome cells of *Artemisia annua*. Mol Plant 12:704–714

Publisher's Note